Surface-Enhanced Raman Scattering of Benzenethiol Adsorbed on Silver-Exchanged Copper Powders

Kuan Soo Shin,[*] Hyunwoo Ryoo,[†] Yoon Mi Lee,[†] and Kwan Kim[†,*]

Department of Chemistry, Soongsil University, Seoul 156-743, Korea. [*]E-mail: kshin@ssu.ac.kr
[†]Department of Chemistry, Seoul National University, Seoul 151-742, Korea. [*]E-mail: kwankim@snu.ac.kr
Received November 26, 2007

Micrometer-sized copper (μCu) powders are weakly surface-enhanced Raman scattering (SERS) active by the excitation at 632.8 nm, but nearly ineffective as a SERS substrate at 514.5 nm excitation. The SERS activity of μCu powders at both excitation wavelengths can be increased dramatically by a simple method of the galvanic exchange reaction with $AgNO_3$ in aqueous medium. In this work, the SERS activity of the Ag-exchanged Cu powders (μCu@Ag) has been evaluated by taking a series of Raman spectra using benzenethiol (BT) as the probe molecule. It is clearly confirmed by field emission scanning electron microscopy and X-ray diffractometry that the SERS activity of μCu@Ag powders is, in fact, highly dependent on the extent of galvanic reaction.

Key Words : Surface-enhanced Raman scattering, Copper powder, Silver dendrite, Galvanic exchange, Benzenethiol

Introduction

Surface-enhanced Raman scattering (SERS) is an abnormal surface optical phenomenon resulting in strongly increased Raman signals from molecules that have been attached to nanometer-sized noble metallic structures. Raman signals arising from molecules adsorbed on Ag nanoparticles can be enhanced by magnitudes up to 10^{14} or 10^{15} times, allowing the detection of single molecules.[1-5] Since its first discovery in the 1970s,[6] SERS has thus been an object of great interest in many areas of science and technology including chemical analysis, corrosion, lubrication, heterogeneous catalysis, biological sensors, and molecular electronics, etc.[7-11]

It has long been believed that two enhancement mechanisms, one called a long-range electromagnetic effect and the other called a short-range chemical effect, are simultaneously operative for SERS, and at least 8-10 orders of magnitude can arise from electromagnetic surface plasmon excitation,[5,12] while the enhancement factor due to the chemical effect is 10^1-10^2 order.[12-15] However, it is still unclear what structural factors are responsible for single-molecule SERS, although an electromagnetic ''hot'' spot is presumed to exist in large fractal Ag aggregates.[16,17] The junction of two aggregated Ag nanoparticles is also presumed to be the ''hot'' site for SERS.[18]

Ever since the discovery of SERS phenomenon, SERS spectra from molecules on silver and gold substrates have been extensively studied. In contrast, copper substrate has received far less attention owing to its inherent instability as well as its relatively weak SERS activity. To use SERS in routine, on-line studies for analytical purposes, SERS spectra should be obtainable even for the molecules anchored on solid surfaces with negligible SERS activity. It is believed that surface Raman spectra can be obtained if Ag or Au nanoaggregates are assembled at the gaps/crevices of organic monolayers. We have recently measured the Raman spectrum of 4-aminobenzenethiol (4-ABT) on powdered Cu substrates with very low signal-to-noise ratios. Dramatic increase in Raman scattering occurred, however, when 4-ABT was sandwiched between Ag/Au nanoparticles and powdered Cu substrates.[19]

The reduction of cations of a metal with a higher reduction potential by a metal with a lower reduction potential is well known. Mengoli *et al.*[20] deposited Ag and Cu on Fe electrodes by dipping the electrodes into aqueous solutions of Ag^+ or Cu^{2+} salts. Nie and Feng[21] produced Ag films on electrolyzed Cu foils and Zuo and Jagodzinski[22] reported a simple method to produce SERS-active metal surfaces (Cd, Ni, Au, Fe, Cu, and Ag) on an Al foil by chemical reduction. More recently, Song *et al.*[23] reported a simple method of the reduction of $AgNO_3$ by copper foil to prepare silver dendrites which could be used as a SERS active substrate. Wen *et al.*[24] also synthesized silver nanodendrites by a simple surfactant-free method using a suspension of Zn microparticles as a reducing agent and showed that Ag nanodenrites provide intense and enhanced Raman scattering.

To observe strong SERS signals, it is indispensable that the analyte molecules have enough adsorption strength to be in direct contact with the SERS-active substrates. It is naturally difficult to observe SERS for molecules weakly adsorbing on the SERS substrates. We intend to observe SERS for molecules adsorbing weakly onto Ag and/or Au substrates. The noble strategy is based on the entrapment of the target analytes inside the pores and gaps of SERS-active nanoaggregates that are supposed to function as the "hot" sites for SERS. The entrapment of the target molecules can be easily accomplished by fabricating SERS-active nanoaggregates *via* the galvanic exchange reaction in the presence of the analytes.[25] Before demonstrating the novel

entrapment method to observe SERS for weakly absorbing molecules, we investigated, in this paper, the SERS characteristics for benzenethiol molecules strongly adsorbed on the silver surface overlaid on micrometer-sized copper powders. The silver-exchanged copper powder was prepared by galvanic exchange reaction using a wide concentration range of aqueous solution of $AgNO_3$; the extent of silver content on copper powder was controlled by changing the concentration of $AgNO_3$.

Experimental

Silver nitrate ($AgNO_3$, 99.8%) was purchased from Junsei. Benzenethiol (BT, 97%), copper powder (3 μm, dendritic, 99.7%), and silver powder (2-3.5 μm, 99.9%) were purchased from Aldrich and used as received. Chemicals otherwise specified were of reagent grade, and highly purified water, of resistivity greater than 18.0 MΩ·cm (Millipore Milli-Q System), was used in making aqueous solutions.

Benzenethiol (BT) adsorbed on copper powder that had previously been subjected to galvanic exchange reaction with silver will be denoted BT/μCu@Ag. To prepare BT/μCu@Ag, the Cu powders were initially washed consecutively with acetone (Merck, >99.5%) and ethanol (Hayman, >99.9%). This process was performed to clean the powders and to remove any carbon impurities on the powders. Secondly, 30 mg of cleaned Cu powder was soaked into 10 mL $AgNO_3$ aqueous solution with different concentrations (from 0.05 to 50 mM). The galvanic exchange reaction was completed within 10 min. The solution phase was decanted and the remaining solid particles were washed with excess water and ethanol. Thirdly, a series of Ag-coated Cu powders was placed in 5 mM ethanolic solution of benzenethiol. After 2 h, the solution phase was decanted and the remaining solid particles were washed with excess ethanol and dried in a vacuum for 2 h, and then subjected to Raman spectral analysis. For a comparative study, the SERS spectra of benzenethiol (BT) adsorbed on pure Cu powders (BT/μCu) as well as on pure Ag powders (BT/μAg) were also measured.

Raman spectra were obtained using a Renishaw Raman system Model 2000 spectrometer equipped with an integral microscope (Olympus BH2-UMA). The 514.5 nm line from a 20 mW Ar^+ laser (Melles-Griot Model 351MA520) and the 632.8 nm line from a 17 mW He/Ne laser (Spectra Physics Model 127) were used as the excitation source. Raman scattering was detected over 180° with a Peltier cooled (−70 °C) charge-coupled device (CCD) camera (400 × 600 pixels). The laser beam was focused onto a sampling spot approximately 1 μm in diameter with an objective microscope with magnification of the order of 20×. The data acquisition time was usually 30 s. The holographic grating (1800 grooves/mm) and the slit allowed the spectral resolution to be 1 cm^{-1}. The Raman band of a silicon wafer at 520 cm^{-1} was used to calibrate the spectrometer, and the accuracy of the spectral measurement was estimated to be better than 1 cm^{-1}.

Field emission scanning electron microscope (FE-SEM) images of silver and copper powders were obtained with a JSM-6700F FE-SEM operated at 5.0 kV. X-ray diffraction (XRD) patterns were obtained on a Rigaku Model D/max-3C powder diffractometer using Cu Kα (1.5419 Å) radiation.

Results and Discussion

The typical FE-SEM images of a series of Ag-exchanged Cu powders (μCu@Ag) obtained by reducing silver ions in the different concentrations of $AgNO_3$ solution with commercially available copper powders are shown in Figure 1. For reference, the images of the original dendritic type Cu powders with a nominal particle size of 3 μm as well as the pure Ag powders with a nominal particle size of 2-3.5 μm are also shown in Figure 1. Following the galvanic exchange reaction, the surface morphology of copper powder is seen to change dramatically. At low concentrations of Ag ion, as shown in Figures 1(b) and 1(c), Ag nanoparticles are formed sparsely on the Cu surface, retaining the dendritic shape of original Cu powders. As the concentration of $AgNO_3$ increases, as shown in Figures 1(d) and 1(e), the Cu powders are fully covered with Ag nanoparticles. Especially, when the concentration of $AgNO_3$ was 50 mM (Figure 1(e)), the dendritic shape of original Cu powders was no longer detected. Instead, Ag nanoparticles seemed to form their

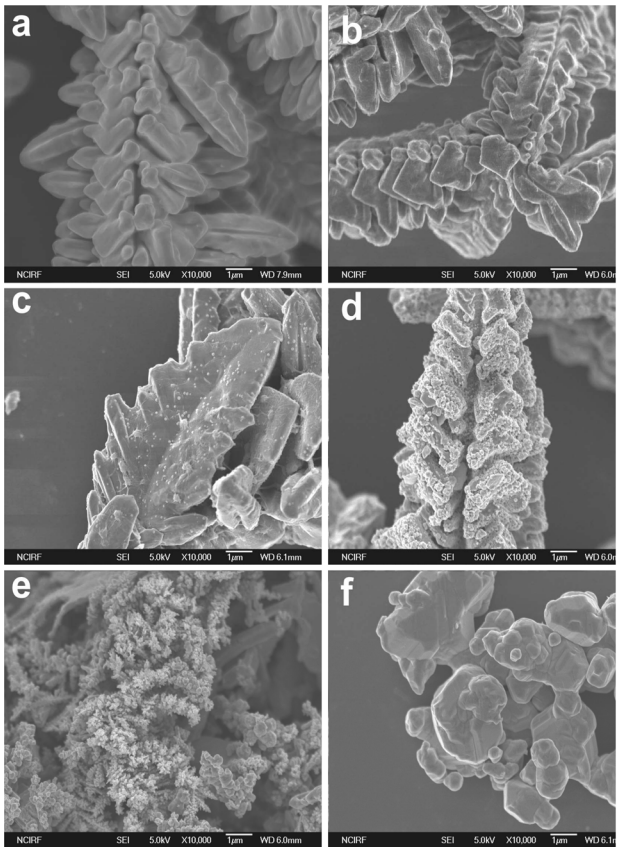

Figure 1. The typical FE-SEM images of (a) pure μCu, (b) μCu@Ag(0.05), (c) μCu@Ag(0.5), (d) μCu@Ag(5), (e) μCu@Ag(50), and (f) pure μAg powders.

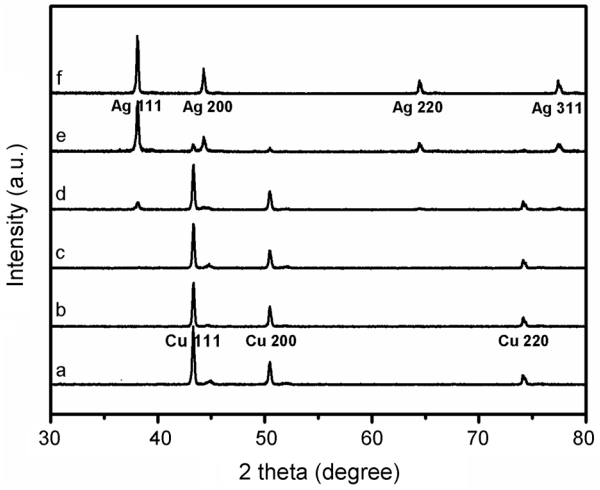

Figure 2. The XRD patterns of (a) pure μCu, (b) μCu@Ag(0.05), (c) μCu@Ag(0.5), (d) μCu@Ag(5), (e) μCu@Ag(50), and (f) pure μAg powders.

own nano-dendrites on the surface of Cu powders. The FE-SEM image of μCu@Ag(50) is obviously different from that of the μAg powders shown in Figure 1(f).

XRD was used to examine the crystal structure of the silver-exchanged copper powder samples. Figure 2 shows the XRD patterns of a series of Ag-exchanged Cu powders; for reference, the XRD patterns of pure Cu and Ag powders are also shown in Figure 2. In fact, the three diffraction peaks of pure Cu powder (Figure 2(a)) can be indexed to the (111), (200), and (220) planes of the face-centered-cubic (fcc) structure of copper. And the four diffraction peaks of pure Ag powder (Figure 2(f)) can also be indexed to the (111), (200), (220), and (311) planes of the fcc structure of silver. It is seen that to observe the XRD peaks of crystalline Ag, the $AgNO_3$ solution must be as concentrated as 5.0 mM (Figure 2(d)). When the concentration of $AgNO_3$ is increased to 50 mM, as shown in Figure 2(e), silver becomes the major component of the Cu/Ag composite powders.

We surmise from the XRD patterns and FE-SEM images that the concentration of $AgNO_3$ solution is the most important factor in the formation of Cu/Ag composite powders by galvanic exchange reaction. This is because much the same XRD patterns and FE-SEM images were reproducibly obtained as long as a galvanic reaction had been conducted at a fixed concentration of $AgNO_3$. In view of these observations and a recent report on the formation of silver nanostructures via a galvanic exchange reaction,[26] the following reaction is anticipated to occur, with copper atoms actively participating as a reducing agent:

$$Cu(s) + 2Ag^{+}(aq) \rightarrow Cu^{2+}(aq) + 2Ag(s) \quad (1)$$

Continuous reduction of Ag ions by Cu atoms requires electron-transfers from the underlying Cu atoms, apart from the concomitant reduction of Ag ions by reducing reagent in solution. At low concentration of $AgNO_3$, reduced silver metal forms nanoparticles over the Cu surface. As the concentration of $AgNO_3$ increases, the Ag nanoparticles

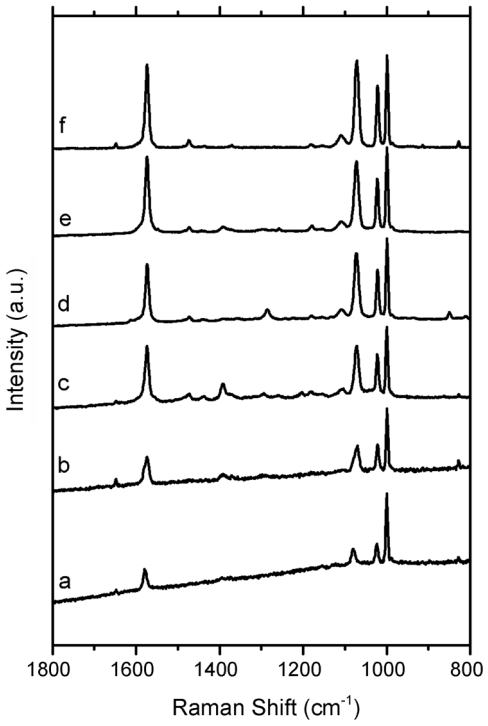

Figure 3. The typical SERS spectra of BT adsorbed on (a) pure μCu, (b) μCu@Ag(0.05), (c) μCu@Ag(0.5), (d) μCu@Ag(5), (e) μCu@Ag(50), and (f) pure μAg powders, respectively. All spectra were obtained using a He/Ne laser at 632.8 nm as the excitation source.

come into being branches, thus forming minute Ag dendrites.

The SERS activity of silver-exchanged copper powders was evaluated by taking SERS spectra using benzenethiol (BT) as the probe molecule. Benzenethiol is a suitable molecule for investigating SERS due to its distinct Raman features and strong affinity for coinage-metal surfaces to form self-assembled monolayers. Figure 3 shows the SERS spectra of BT adsorbed on a series of Ag-exchanged Cu powders (BT/μCu@Ag) taken using a He/Ne laser at 632.8 nm as the excitation source. For reference, the Raman spectrum of BT on pure Cu powders, as well as that on pure Ag powders, is also shown in Figure 3. As can be seen in Figure 3(a), a distinct spectrum is observed for BT adsorbed on pure Cu powders. The bands at 999, 1022, 1072, and 1574 cm^{-1} in Figure 3(a) can be assigned to the in-plane ring-breathing mode, the in-plane C-H bending mode, the in-plane ring-breathing mode coupled with the C-S stretching mode, and the C-C stretching mode, respectively.[27] As the concentration of $AgNO_3$ is increased gradually from 0.05 to 50 mM to obtain Ag-exchanged Cu powders, the intensities of SERS peaks of BT are dramatically increased, as can be seen in Figures 3(b) to 3(e).

Changes in the relative peak intensities in Figures 3(a) to 3(e) are probably due to differences in the orientation of BT with respect to the surfaces. Particularly noteworthy is the noticeable difference between the relative peak intensities at 999, 1022, and 1072 cm^{-1} on pure Cu and those on pure Ag.

A gradual variation in relative intensity of these bands in Figures 3(a) to 3(e) may then be associated with the concomitant changes in the surface metal composition. It is unfortunate that all these bands are assigned as a_1 modes,[28] rendering an exact orientation analysis impossible; however, on the basis of surface Raman selection rules, the data suggest that the aromatic ring is oriented largely perpendicular to these surfaces.[29] A similar qualitative argument was presented by Carron *et al*.[30] for the perpendicular orientation of the aromatic ring of BT at nitric acid-etched Ag foil surfaces. To see more clearly the concentration effect of $AgNO_3$ in the galvanic exchange reaction, in Figure 4 are plotted the relative Raman intensities of BT at 1574 cm^{-1} adsorbed on μCu, μCu@Ag(0.05), μCu@Ag(0.5), μCu@Ag(5), μCu@Ag(50), and μAg powders. It is seen that the relative Raman intensities of BT increase as the extent of Ag component in the powders increases. There thus exists a strong correlation between the SERS activity and the composition of Ag. The relative enhancement factors (REFs) for the 8a band at 1574 cm^{-1} of the BT on six powders, *i.e*. μCu: μCu@Ag(0.05): μCu@Ag(0.5): μCu@Ag(5): μCu@Ag(50): μAg powders, are approximately 1:2.8:14:52:113:826.

The surface enhancement factor (EF) of BT on Ag powder was estimated by using the following relationship:[31]

$$EF = (I_{SERS}/I_{NR})(N_{NR}/N_{SERS}) \quad (2)$$

in which I_{SERS} and I_{NR} are the SERS intensity of BT on Ag powders (shown in Figure 3(f)) and the normal Raman (NR) intensity of BT in bulk, respectively, and N_{SERS} and N_{NR} are the number of BT molecules illuminated by the laser light to obtain the corresponding SERS and NR spectra, respectively. I_{SERS} and I_{NR} were measured for the 8a band of BT at 1574 cm^{-1}, and N_{SERS} and N_{NR} were calculated on the basis of the estimated concentration of the surface BT species, surface roughness of the Ag powders, density of bulk BT, and the sampling areas. Taking the sampling area (*ca*. 1 μm in diameter), the coverage of BT (0.71 nmol cm^{-2}),[32] and the roughness factor of Ag particles (*ca*. 1.3) which was estimated from the AFM images and the FE-SEM images (Figure 1(f)) into account, $N_{SERS} = 4.4 \times 10^6$. When taking the NR spectrum of solutions of BT, the sampling volume will be the product of the laser spot (*ca*. 1 μm in diameter) and the penetration depth of the focused beam (*ca*. 75 μm); since the density of BT solution used is 1.07 g cm^{-3}, N_{NR} is then to be 4.2×10^{11}. Finally, the intensity ratio, I_{SERS}/I_{NR}, was measured to be ~7.98 so that the EF value of BT on Ag powders using 632.8 nm radiation as an excitation source should be ~7.7×10^5. The EF values of the BT on μCu, μCu@Ag(0.05), μCu@Ag(0.5), μCu@Ag(5), and μCu@Ag(50) powders derived from the relative enhancement factors at 1574 cm^{-1} at 632.8 nm excitation are then 9.3×10^2, 2.6×10^3, 1.3×10^4, 4.8×10^4, and 1.1×10^5, respectively.

For comparing the relative SERS activity along the excitation wavelength, we have also performed SERS measurements using an Ar^+ laser (514.5 nm) as the excitation source. Figure 5 show a series of SERS spectra of BT adsorbed on a series of Ag-exchanged Cu powders (BT/μCu@Ag). The overall changes of Raman intensities and spectral features are much the same as those observed using a He/Ne laser (632.8 nm) as the excitation source. However, as shown in Figure 5(a), we could not obtain any discernable SERS spectrum for BT adsorbed on pure Cu powders by using 514.5 nm radiation as the excitation source. This is presumed due to the fact that the surface plasmon resonance wavelength of Cu powders is located at >514.5 nm. Upon

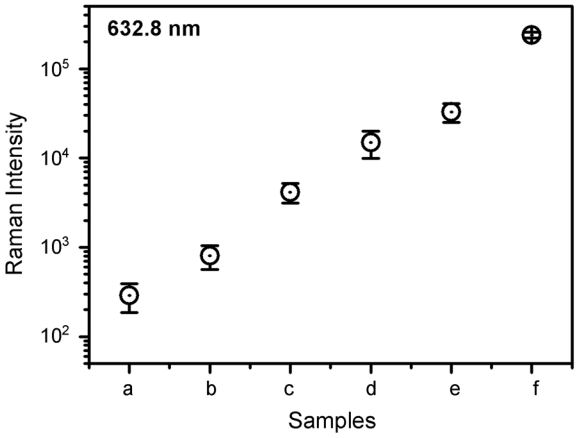

Figure 4. Relative Raman intensities of BT at 1574 cm^{-1} adsorbed on (a) pure μCu, (b) μCu@Ag(0.05), (c) μCu@Ag(0.5), (d) μCu@Ag(5), (e) μCu@Ag(50) and (f) pure μAg powders, respectively. Raman scattering intensities are the average of 5 measurements.

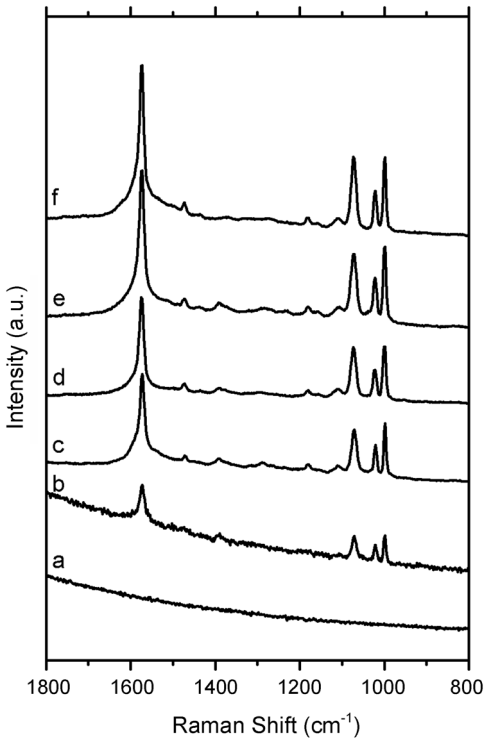

Figure 5. The typical SERS spectra of BT adsorbed on (a) pure μCu, (b) μCu@Ag(0.05), (c) μCu@Ag(0.5), (d) μCu@Ag(5), (e) μCu@Ag(50), and (f) pure μAg powders, respectively. All spectra were obtained using an Ar ion laser at 514.5 nm as the excitation source.

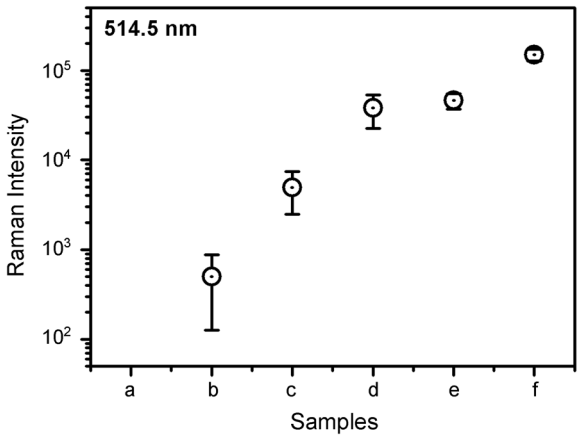

Figure 6. Relative Raman intensities of BT at 1574 cm^{-1} adsorbed on (a) pure μCu, (b) μCu@Ag(0.05), (c) μCu@Ag(0.5), (d) μCu@Ag(5), (e) μCu@Ag(50) and (f) pure μAg powders, respectively. Raman scattering intensities are the average of 5 measurements.

the deposition of Ag onto the Cu powder by a galvanic exchange reaction, the Raman peaks of BT are clearly identified, however. To see this more quantitatively, in Figure 6 are shown the relative Raman intensities of the 8a band at 1574 cm^{-1} of the BT on μCu, μCu@Ag(0.05), μCu@Ag(0.5), μCu@Ag(5), μCu@Ag(50) and μAg powders obtained using an Ar^+ laser (514.5 nm) as the excitation source. It is obvious that the relative Raman intensities increase as the composition of Ag increases. The relative enhancement factors for the 8a band at 1574 cm^{-1} of the BT on five powders, *i.e.*, μCu@Ag(0.05): μCu@Ag(0.5): μCu@Ag(5): μCu@Ag(50): μAg powders are approximately 1:9.8:76:91:298. Considering the fact that the absolute surface enhancement factor of BT (at 1574 cm^{-1}) on pure Ag powders at 514.5 nm excitation is estimated to be ~4.8×10^5, the corresponding EF values of BT on μCu@Ag(0.05), μCu@Ag(0.5), μCu@Ag(5), and μCu@Ag(50) powders at 514.5 nm excitation may then be 1.6×10^3, 1.6×10^4, 1.2×10^5, and 1.5×10^5, respectively.

Conclusions

We have investigated the galvanic exchange reaction of micrometer-sized copper (μCu) powders with silver ions. The reaction was completed within 10 min at room temperature. At lower concentration, Ag nanoparticles were sparsely formed on the copper powders. Increasing the silver ion concentration, dendritic Ag nanostructures were finally formed onto Cu. Although pure Cu powders were quite ineffective as a SERS substrate, the galvanic exchanged powders exhibited as much SERS activity as pure Ag powders, owing to the formation of dendritic Ag nanostructures; the EF value estimated using BT as a probe molecule has thus reached, for instance, 1.5×10^5 for 514.5 nm excitation and 1.1×10^5 for 632.8 nm excitation. The present observation suggests that galvanic exchange reaction of copper with silver ions is a promising methodology not only to enlarge the optoelectronic application of copper powders but also to entrap the target analytes inside the pores and gaps of SERS-active nanoaggregates that are supposed to function as the hot sites for SERS.

Acknowledgement. This work was supported by the Korea Science and Engineering Foundation (Grant R01-2006-000-10017-0 and R11-2007-012-02002-0). KSS was also supported by the Soongsil University Research Fund.

References

1. Nie, S.; Emory, S. R. *Science* **1997**, *275*, 1102.
2. Kneipp, K.; Wang, Y.; Kneipp, H.; Perelman, L. T.; Itzkan, I.; Dasari, R. R.; Feld, M. S. *Phys. Rev. Lett.* **1997**, *78*, 1667.
3. Kneipp, K.; Kneipp, H.; Itzkan, I.; Dasari, R. R.; Feld, M. S. *Chem. Rev.* **1999**, *99*, 2957.
4. Xu, H.; Bjerneld, E. J.; Käll, M.; Börjesson, L. *Phys. Rev. Lett.* **1999**, *83*, 4357.
5. Futamata, M.; Maruyama, Y.; Ishikawa, M. *Vib. Spectrosc.* **2002**, *30*, 17.
6. Fleischmann, M.; Hendra, P. J.; McQuillan, A. J. *Chem. Phys. Lett.* **1974**, *26*, 163.
7. Ni, J.; Lipert, R. J.; Dawson, G. B.; Porter, M. D. *Anal. Chem.* **1999**, *71*, 4903.
8. Kim, N. H.; Lee, S. J.; Kim, K. *Chem. Commun.* **2003**, *9*, 724.
9. Tian, Z. Q.; Ren, B.; Wu, D. Y. *J. Phys. Chem. B* **2002**, *106*, 9463.
10. Lee, C. J.; Kim, H. J.; Karim, M. R.; Lee, M. S. *Bull. Korean Chem. Soc.* **2006**, *27*, 545.
11. Joo, S.-W. *Bull. Korean Chem. Soc.* **2007**, *28*, 1405.
12. Jiang, J.; Bosnick, K.; Maillard, M.; Brus, L. *J. Phys. Chem. B* **2003**, *107*, 9964.
13. Lecomte, S.; Matejka, P.; Baron, M. H. *Langmuir* **1998**, *14*, 4373.
14. Campion, A.; Ivanecky, J. E.; Child, C. M.; Foster, M. *J. Am. Chem. Soc.* **1995**, *117*, 11807.
15. Doering, W. E.; Nie, S. *J. Phys. Chem. B* **2002**, *106*, 311.
16. Markel, V. A.; Shalaev, V. M.; Zhang, P.; Huynh, W.; Tay, L.; Haslett, T. L.; Moskovits, M. *Phys. Rev. B* **1999**, *59*, 10903.
17. Bozhevolnyi, S. I.; Markel, V. A.; Coello, V.; Kim, W.; Shalaev, V. M. *Phys. Rev. B* **1998**, *58*, 11441.
18. Michaels, A. M.; Jiang, J.; Brus, L. *J. Phys. Chem. B* **2000**, *104*, 11965.
19. Kim, K.; Lee, H. S. *J. Phys. Chem. B* **2005**, *109*, 18929.
20. Mengoli, G.; Musiani, M. M.; Fleischman, M.; Mao, B.; Tian, Z. Q. *Electrochim. Acta* **1987**, *32*, 1239.
21. Nie, C.-S.; Feng, Z. *Appl. Spectrosc.* **2002**, *56*, 300.
22. Zuo, C.; Jagodzinski, P. W. *J. Phys. Chem. B* **2005**, *109*, 1788.
23. Song, W.; Cheng, Y.; Jia, H.; Xu, W.; Zhao, B. *J. Colloid Interface Sci.* **2006**, *298*, 765.
24. Wen, X.; Xie, Y.-T.; Mak, M. W. C.; Cheung, K. Y.; Li, X.-Y.; Renneberg, R.; Yang, S. *Langmuir* **2006**, *22*, 4836.
25. Yosef, I.; Avnir, D. *Chem. Mater.* **2006**, *18*, 5890.
26. Qu, L.; Dai, L. *J. Phys. Chem. B* **2005**, *109*, 13985.
27. Joo, T. H.; Kim, M. S.; Kim, K. *J. Raman Spectrosc.* **1987**, *18*, 57.
28. Carron, K. T.; Hurley, L. G. *J. Phys. Chem.* **1991**, *95*, 9979.
29. Taylor, C. E.; Pemberton, J. E.; Goodman, G. G.; Schoenfisch, M. H. *Appl. Spectrosc.* **1999**, *53*, 1212.
30. Xue, G.; Ma, M.; Zhang, J.; Lu, Y.; Carron, K. T. *J. Colloid Interface Sci.* **1992**, *150*, 1.
31. Yu, H. Z.; Zhang, J.; Zhang, H. L.; Liu, Z. F. *Langmuir* **1999**, *15*, 16.
32. Wan, L.-J.; Terashima, M.; Noda, H.; Osawa, M. *J. Phys. Chem. B* **2000**, *104*, 3563.